REGULAR PAPER

Gait Training Algorithm of an End-Effector Typed Hybrid Walking Rehabilitation Robot

Jung-Yup Kim[1] · Jung-Joon Kim[1] · Kiwon Park[2]

Abstract

The present study focused on the gait training algorithm of an end-effector typed hybrid walking rehabilitation robot that our research group developed in 2017. One motor and five link mechanism in the end-effector typed hybrid walking rehabilitation robot were used to mimic normal gait patterns. Depending on patients' condition and training difficulty, three gait rehabilitation training modes were proposed. Mode 1 is a passive mode that motor leads to patients' walking entirely, Mode 2 is an assisted-active mode that a part of patients' muscle strength were supported depending on their walking intention, and Mode 3 is an active mode that patients walk on their own muscle strength under gait resistance by eddy current brake. At each training mode, patients' muscle strength performance by driving motor was experimentally verified using electromyography. In addition, gait symmetry between injured limb and uninjured limb improved as evidenced by motion capture analysis using inertial measurement unit.

Keywords Walking rehabilitation · Gait training · EMG experiment
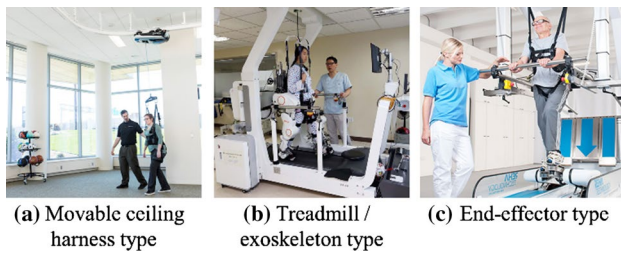
1 Introduction

Decrease in birth rate and increase in life expectancy around the world lead to an aging population, which causes various social problems. The elderly's quality of life has been declining due to the decrease in their physical function and physical activity [1], and the risk of walking disorders caused by stroke, Parkinson's disease, etc. have also been increasing [2, 3]. In the case of stroke, it is effective to start rehabilitation as early as possible and continue for a long time [4, 5]. However, it is difficult to receive good quality rehabilitation treatment from lack of physical therapist and rehabilitation infrastructure. In order to solve these social problems, researches on gait rehabilitation have been actively carried out [6–9] and robot technology begin to attract attention as a solution.

These gait rehabilitation robots can be divided into three types: portable ceiling harness type, treadmill/exoskeleton type, and end-effector type (Fig. 1). ZeroG of American ARETECH Corporation is representative for portable ceiling harness type [10]. This gait rehabilitation robot supports the weight of the patient by using the cable and the upper harness. However, the physical therapist must induce the patient to walk because the patient does not move his/her lower limb joints while using this rehabilitation robot. Therefore, it is difficult for patients to exercise regularly with this type of robot. The treadmill/exoskeleton type robots are Lokomat [11] from Hocoma of Switzerland and Walkbot [12] from P&S Mechanics. Patients wear an exoskeleton type robot that surrounds their lower limbs. However, since the entire lower limb is fixed to the robot, patients' motions are limited during rehabilitation exercise which may make them be more passive. Furthermore, it is difficult to be widely available due to its bulkiness, heaviness, and expensive price. End-effector type robots are typically REHA Technology's G-EO System [13]. The characteristic of the robot is that only patients' feet are fixed to the robot arm, not the entire lower limb. This feature enables the patients to maintain the degree of freedom while gait rehabilitation training. However, there is a risk that the patient may be injured by the
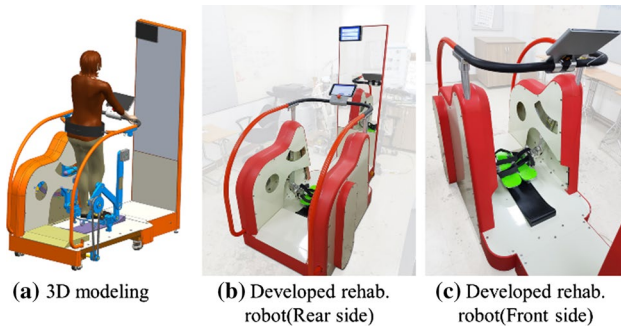
✉ Kiwon Park
  kiwon@inu.ac.kr

[1] Department of Mechanical System Design Engineering, Seoul National University of Science and Technology, Seoul 01811, South Korea

[2] Department of Mechatronics Engineering, Incheon National University, Incheon 22012, South Korea

(a) Movable ceiling harness type　**(b)** Treadmill / exoskeleton type　**(c)** End-effector type

Fig. 1 Three types of walking rehabilitation robots

(a) Optimized 5-link mechanism & floor　**(b)** 3D mechanical design

Fig. 3 Proposed 5-link mechanism and curved floor

(a) 3D modeling　**(b)** Developed rehab. robot(Rear side)　**(c)** Developed rehab. robot(Front side)

Fig. 2 Developed end-effector typed walking rehabilitation robot

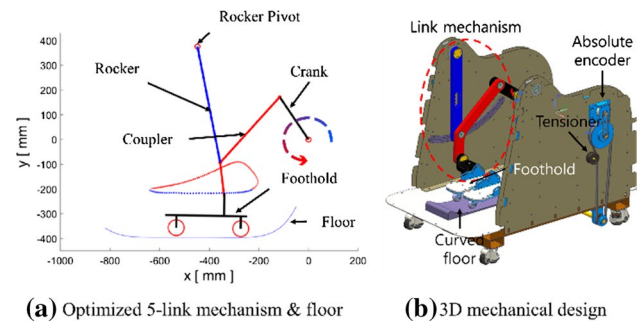**Fig. 4** 3D modeling of hybrid driving system

malfunction of the robot arm mounted on both feet, and it is bulky and heavy.

We present a gait rehabilitation robot that solves the disadvantages of existing rehabilitation robots from 2017 and is easier to supply shown in Fig. 2 [14]. The robot has an end-effector type to guarantee the degree of freedom of the patient and the cost, volume and weight are minimized by driving the five link mechanism which implements the walking trajectory with only one motor. In addition, there is an advantage that an active type exercise capable of walking only by a patients' strength is available. A parallel type hybrid drive unit in a robot uses a freewheel that allows only a single direction rotation to separate a driving force of a patient from a driving force of a motor.
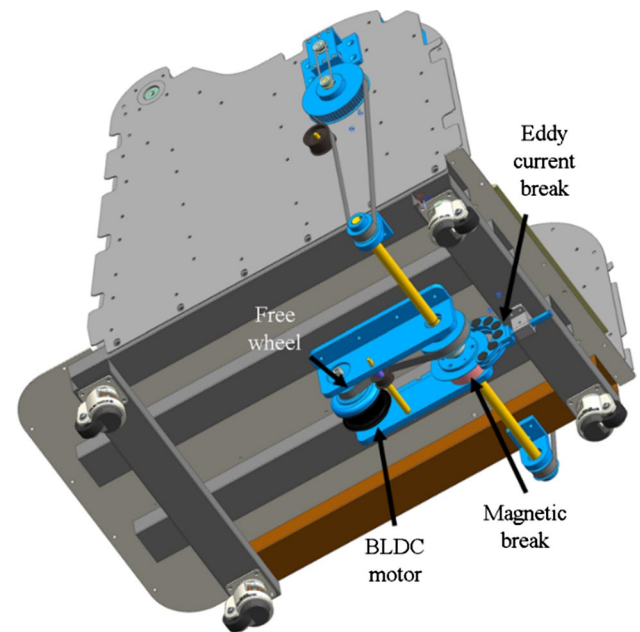
In this paper, we briefly introduced the hardware of end-effector type walking rehabilitation robots recently developed by our research group, and proposed three gait training modes designed for gait rehabilitation. Finally, the performance of gait training modes was evaluated by examining patients' muscle activation and their captured motion data.

2 Overview of Our Walking Rehabilitation Robot

In this section, we briefly introduced the gait rehabilitation robot that we recently developed. The most prominent feature is the 5-bar link mechanism and curved floor that

mimics ankle positon and angular displacement of normal gait patterns based on the recorded motion capture data and optimization technique (Fig. 3). This 5-bar link mechanism has the advantage that normal gait pattern can be completely generated even by a single motor rotating the crankshaft. A freewheel that allows only one-directional rotation is mounted on the motor driving part. In order to operate 5-bar link mechanism, superimposing the motor driving force and patients' muscle force was used for parallel hybrid driving part (Fig. 4). In addition, the rotation of the crankshaft can be fixed using a magnetic brake for safe entry and exit of the patient. An eddy current brake consisting of a magnet and a disk was fabricated and then attached to the drive shaft, thereby allowing resistance to movement of the link. It enables to generate ground friction of their sole that people experience during walking (Fig. 5). Angular displacement, velocity and acceleration of the crankshaft were measured

Fig. 5 3D modeling of eddy current break system

Table 1 Specifications of developed walking rehabilitation robot

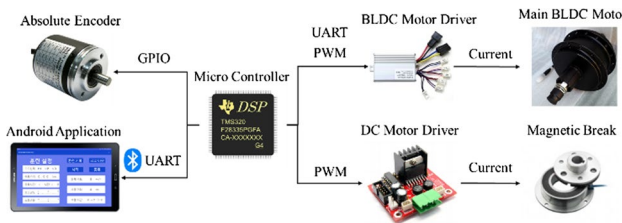| Weight	311 kgf
Size	1810×946×1962 mm
Training mode	Passive, assisted-active and active
Actuators	Geared BLDC motor + timing pulley/belt
Sensors	Absolute encoder
Controllers	Main controller: TMS320F28335
	BLDC motor controller, magnetic break controller

Fig. 6 Control system diagram

by an attached absolute encoder to the crankshaft in order to detect the patients' walking intention. Table 1 shows the overall specifications of the robot.

Figure 6 represents the control system of the designed robot using the TMS320F28335 microcontroller from Texas Instrument (TI) that performs four functions, (1) the speed control of the BLDC motor, (2) ON/OFF control of the magnetic brake, (3) the measurement of the absolute encoder, and (4) the operation command reception and the walking information transmission through the tablet PC. Specifically, the speed control of the BLDC motor and the ON/OFF control of the magnetic brake are performed by using the pulse width modulation (PWM) signal, and the angular displacement of the absolute encoder is detected by using the general purpose input/output (GPIO). In addition, data transmission/reception between the tablet PC and the microcontroller is performed using Bluetooth communication.
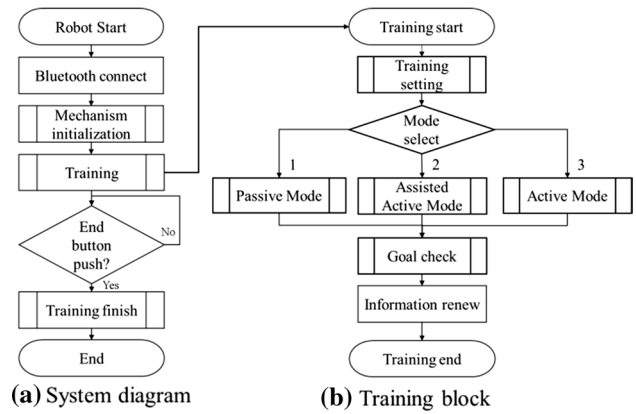

(a) System diagram   **(b)** Training block

Fig. 7 Operation flow chart of the robot

Figure 7 represents the operation flowchart of the robot. First, a mechanism initialization is performed so that the patient can stably ride on the robot. This drives the 5-bar link mechanism so that the patients' pre-set foot of the affected limb is located at the mechanical top dead center and the foot of the unaffected limb is positioned at the mechanical bottom point. Therefore, the patients support the entire body weight with their unaffected limbs so that stable boarding is possible. The training is divided into three modes (passive, assisted-active, active), and training is performed based on walking target speed, distance and time to the tablet PC in the training setting. The detailed features of the three modes are described in the next chapter. When the training is finished, the mechanism is initialized again. To date, the training situation is recorded and stored, and the training information is displayed on the tablet PC so that the user can check the training contents.

3 Three Gait Training Modes

The robot developed in this study has three modes as briefly explained in the previous chapter. In the passive mode, gait rehabilitation is performed only by the driving force of the motor. In the active mode, gait rehabilitation is performed only by patients' muscle forces. In the assisted-active mode, gait rehabilitation is performed by using both the motor and patients' muscle forces simultaneously. In particular, the existing end-effector type or treadmill/exoskeleton type gait rehabilitation robots do not have active mode, but the present robot has the merit that walking rehabilitation training can be performed only by patients' muscle forces.

3.1 Passive Mode

The passive mode is designed to allow patients who have started gait training to become accustomed to and to be
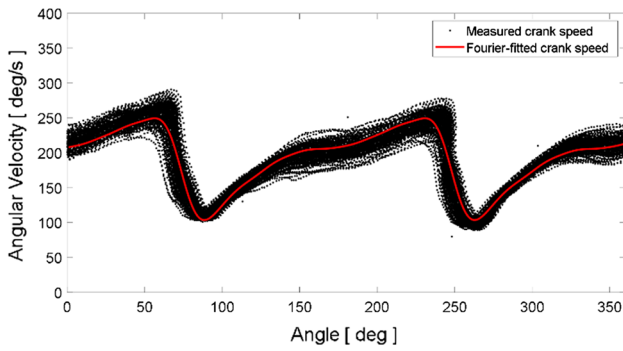
Fig. 8 Crank speed trajectory and its fitted trajectory during slow walking at 2 km/h
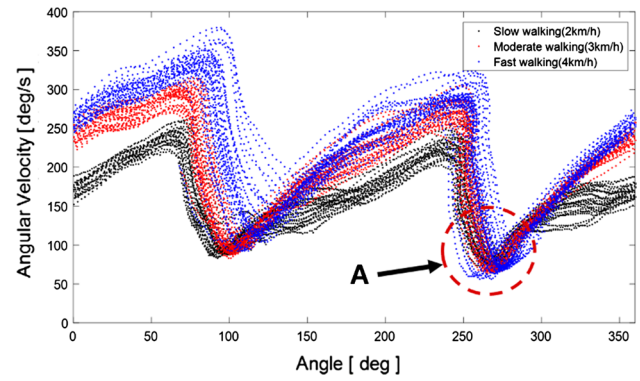

Fig. 9 Measured crank speed trajectories at various walking speeds

Table 2 Coefficients of Fourier-fittings

Parameter	a_0	a_1	a_2	a_3	a_4
Value	191.9	34.78	−27.15	14.03	−8.255
Parameter	a_5	a_6	a_7	a_8	
Value	3.342	−0.8211	−0.3377	0.4076	
Parameter	b_1	b_2	b_3	b_4	b_5
Value	33.01	−14.85	0.5377	2.705	−2.897
Parameter	b_6	b_7	b_8	ω	
Value	1.87	−0.6954	0.2338	0.03604	

Fig. 10 Generated crank speed trajectories $F_P(\theta_c)$ at various walking speeds

able to memorize and repeat the normal gait patterns, while at the same time increasing the leg strength to support the weight. The key to this mode is the speed at which the crankshaft of the 5-bar link mechanism rotates. This is because the end-position trajectory of the 5-bar link mechanism follows the ankle position trajectory of the normal person, but the end-speed trajectory changes depending on the rotational speed of the crankshaft. Therefore, when a normal people walk slowly at a speed of 2 km/h in accordance with the general walking speed of patients in gait rehabilitation program, the angular velocity of the crankshaft is measured through an absolute encoder (Fig. 8). Based on the data from the encoder, the angular velocity profile of the crankshaft that follows the ankle velocity trajectory of the normal people is approximated using Fourier function as Eq. (1). The parameters of the corresponding equation are summarized in Table 2 (see the red trajectory in Fig. 8).
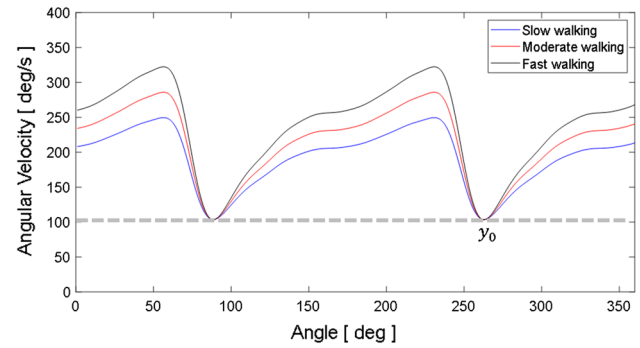
$$f(\theta_c) = a_0 + \sum_{i=1}^{8}\left\{a_i \cos\left(i\omega\theta_c\right) + b_i \sin\left(i\omega\theta_c\right)\right\} \quad (1)$$

where θ_c is an angular displacement of the crankshaft.

The angular velocity trajectory of the crankshaft was also measured when walking faster. The results from the experiment showed that even if the walking speed changes, the angular velocity of the crankshaft at the lowest speed (part A) did not change significantly, and the amplitude of the angular velocity trajectory increased in proportion to the walking speed (Fig. 9). Therefore, in order to generate the angular velocity profile of the crankshaft according to the walking speed set by the patient, the minimum angular velocity y_0 is eliminated from $f(\theta_c)$ (Eq. 2). The gain k_f based on the walking speed V_w set as shown in Eq. (4) is multiplied, and the crankshaft angular velocity profile based on the set walking speed is added by the minimum speed to the Eq. (3). Figure 10 represents the angular velocity trajectory of the crankshaft obtained in Eq. (3).

$$f_0(\theta_c) = f(\theta_c) - y_0 \quad (2)$$

$$F_P(\theta_c) = k_f f_0(\theta_c) + y_0 \quad (3)$$

$$k_f = 20(V_w - 2.0) \quad (4)$$

3.2 Assisted-Active Mode

In the assisted-active mode, the robot grasps the patient's walking intention based on the angular velocity and acceleration data of the crankshaft, and changes the driving speed of the motor depending on the patient's walking intention. The motor driver controls the speed of the motor by applying the command voltage corresponding to the required motor speed to the motor driver. Although gait training at a high speed is advantageous for rehabilitation and strengthening muscles [15, 16], patients with stroke or Parkinson's disease often lack sufficient strength for faster walking. In this case, patients are able to perform gait training at a faster speed with less muscle power using the assisted-active mode.

In order to determine the speed change of the motor based on the patient's walking intention, in this mode, a method of increasing the speed of the motor in proportion to the walking intention based on the angular velocity profile proposed in passive mode is used. The walking speed intention (I_v) and the walking acceleration intention (I_a) are calculated from the angular speed $F_P(\theta_c)$, the angular acceleration $\dot{F}_P(\theta_c)$ of the crankshaft determined based on the walking speed set by the patients, and the actual angular velocity ($\dot{\theta}_c$) and acceleration ($\ddot{\theta}_c$) of the crankshaft [Eqs. (5) and (6)]. Difference in the angular velocity of the crankshaft reflects the patient's acceleration / deceleration intention, and difference in the angular velocity of the crankshaft represents the patient's normal walking speed intention. The calculated I_v and I_a are multiplied by the appropriate proportional coefficient, and each term is added to calculate the walking intention I_T [Eq. (7)]. Finally, the crank angular velocity profile $F_A(\theta_c)$ driven by the motor in assisted-active training mode were proposed from the on-line gait intention I_T, the predetermined velocity gain k_f and the lowest velocity y_0 in the Passive Mode [Eq. (8)].

$$I_v = \dot{\theta}_c - F_P(\theta_c) \tag{5}$$

$$I_a = \ddot{\theta}_c - \dot{F}_P(\theta_c) \tag{6}$$

$$I_T = k_v I_v + k_a I_a \tag{7}$$

$$F_A(\theta_c) = (1 + I_T) k_f f_0(\theta_c) + y_0 \tag{8}$$

In order to verify the generated angular velocity profile of motor based on the proposed gait intention in this training mode, we performed slow walking with low walking intention (A) and fast walking with high walking intention (B) (Fig. 11). Figure 11a shows the angular velocity of the crankshaft measured by the encoder, and Fig. 11b is a graph of the corresponding angular velocity of the motor. In the section A of Fig. 11a, the patient has less intent
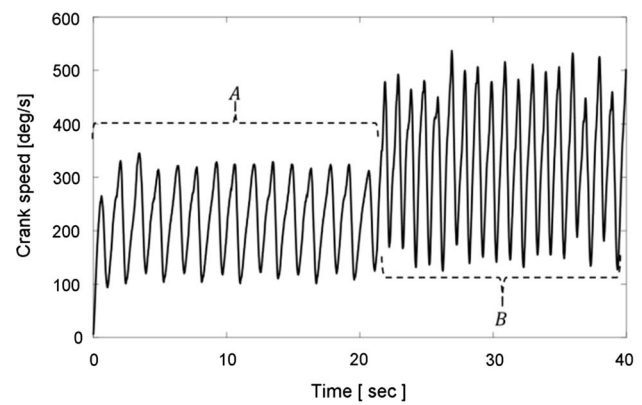
(a) Measured crank speed trajectory
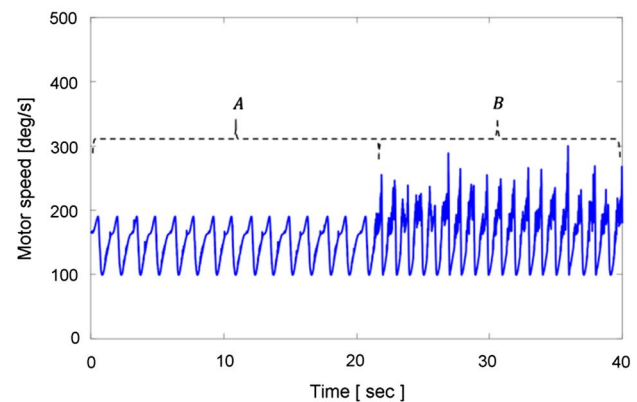
(b) Motor speed trajectory

Fig. 11 Generated motor speed trajectory according to the walking intention of the user during assisted-active mode

to walk. It can be seen that the amplitude of the angular velocity trajectory of the motor is constant (Fig. 11b). Conversely, in the section B, the rotational speed of the crank increased as the walking intention is relatively high, and the amplitude of the angular velocity profile of the motor immediately increased.

3.3 Active Mode

The active mode is a training mode in which the motor does not provide additional muscle aids to the patient's gait and only trains the gait with the patient's own muscle strength. As mentioned above, the developed robot is equipped with an eddy current brake, so the user is able to control the walking resistance. Therefore, in this training mode, the angular velocity profile of a motor is not required, but the position of the eddy current brake is adjusted to appropriately adjust the walking training intensity.

4 Walking Experiments

To examine the performance of the three training modes proposed above, two kinds of gait experiments were conducted. The first is the Electromyography (EMG) signal measurement experiment, which quantify the decrease in the user's lower leg strength according to the motor assist. The second is the lower extremity motion capture experiment using the Inertial Measurement Unit (IMU) sensor (see a video [17]). In the Assisted-active training mode, gait symmetry of lower extremity motion was investigated. Twenty-six-year-old non-disabled person with a height and weight of 179 cm, 75 kg participated in this gait experiment. The subject signed an informed consent and approval was obtained from Seoul National University of Science and Technology Institutional Review Board.

4.1 EMG measurement test

In order to measure muscle strength during walking, EMG sensors were attached to the four muscles of the lower limb (Fig. 12). The selected muscles were Tibialis anterior, Quadriceps femoris (Rectus femoris), Triceps surae (Gastrocnemius), Hamstrings, and the mean integrated EMG values measured on a total of eight sensors during walking were used. The subject walked at a speed of 3 km/h for 1 min. Three trials were performed for each training mode and the mean values of Integrated EMG signal were recorded. Figure 13 represent the trajectories of the integrated EMG signals in each training mode, and the average values of those trajectories were recorded in Table 3. As shown in Fig. 13 and Table 3, it was found that most leg muscles were used in the Active mode without motor assist, and the lowest leg muscles were used in the Passive mode using only the driving force of the motor. In the assisted-active mode, it was
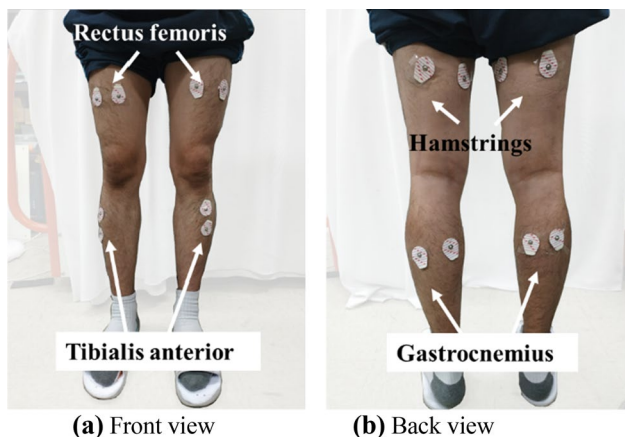

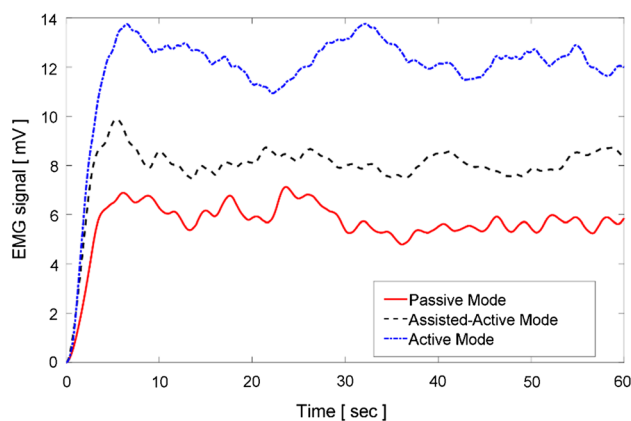**Fig. 12** Selected muscles and locations of EMG sensors

Fig. 13 Comparison of EMG signals in three training modes

found that lower leg muscle was used halfway between the Passive mode and the Active mode as expected. This results suggest that the motor performs correctly the assist of the user's lower extremity muscle strength, and it is possible to increase gradually the muscle use amount in the Passive mode, Assisted-active mode and Active mode order when the patient performs gait rehabilitation training.

4.2 Motion Capture Test Using IMU sensors

To investigate how the robot improves the patient's lower extremity motion during gait in the Assisted-Active mode, lower limb motions were recorded using IMU sensors. As explained in the Sect. 4.1., the subject (height: 179 cm, mass: 75 kg, age: 26 years old) who does not have any neurological and musculoskeletal injuries that might affect gait participated in the experiment. To simulate knee joint injury, the subject wore a brace on the right knee which would restrict the knee range of motion (Fig. 14). IMU sensors were attached to thigh, shank, and foot (Fig. 14). Hip, knee, and ankle joint angles were calculated from the data collected using IMU sensors (Fig. 15).

The subject walked on the developed robot both in the assisted-active mode and the active mode, and three trials were performed for each mode. In the assisted-active mode, the robot helps the subject walk by driving a motor while in the active mode the subject does not receive any types of help from a motor.

Table. 3 Averaged EMG signal values of the three training modes

	Passive mode	Assisted-active mode	Active mode
Averaged signal (mV)	5.8562	8.1919	12.3101

(a) Front view　　　**(b)** Side view
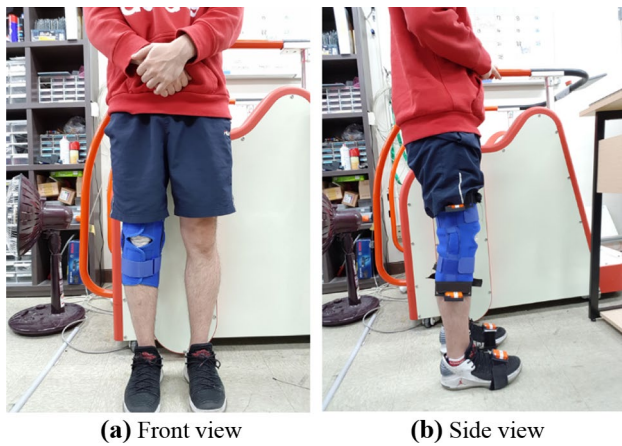
Fig. 14 The subject who wore the knee brace and IMU in the right leg

Fig. 15 Definition of the joint angles

Fig. 16 Average left and right knee angle in the assisted-active mode
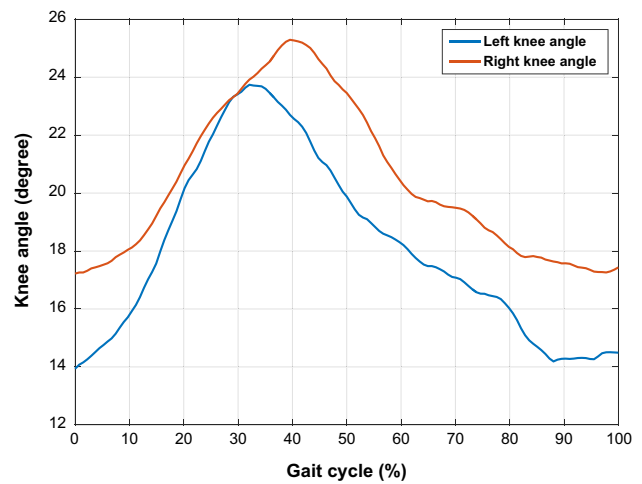
Fig. 17 Average left and right knee angle in the active mode
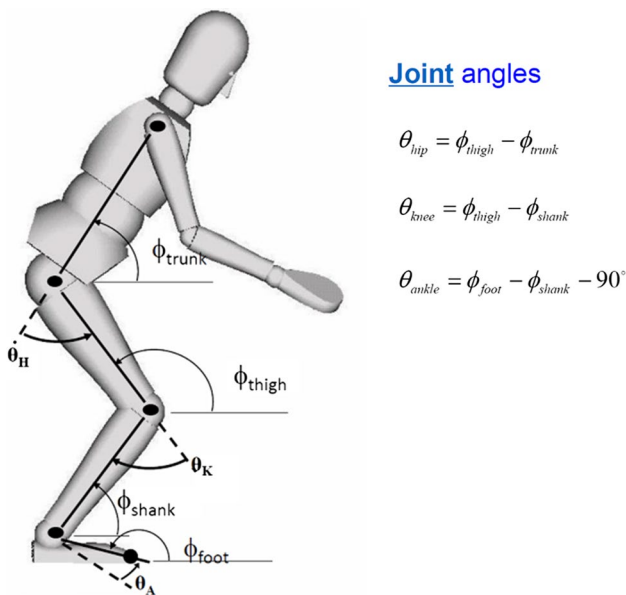
To qualitatively assess bilateral asymmetry, the knee angular displacements from human subject have been collected experimentally, and were averaged over successive gait cycles for both the assisted-active mode and the active mode. In the assisted-active mode that a motor provides additional force, the patient showed higher symmetry during walking on the robot than in the active mode without motor driving forces. In addition, the averaged knee angle trajectories tend to be smoother in the assisted-active mode than in the active mode (Figs. 16, 17).

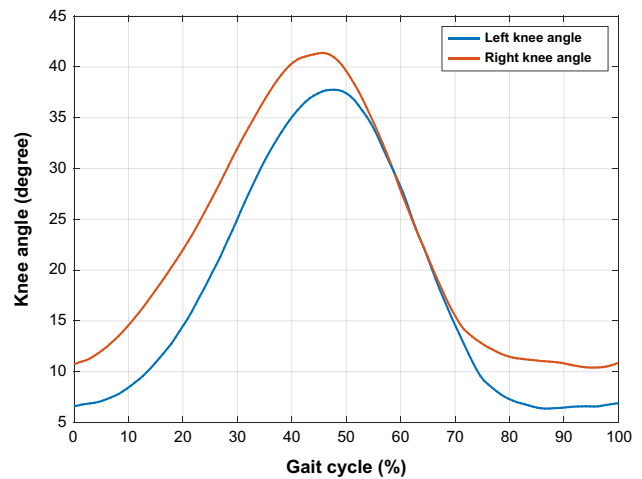Normal human gait patterns are often assumed to be laterally symmetric which means motions in both right and left sides are identical in the sagittal plane [18]. In order to examine lateral gait symmetry, the cross-correlation that measures similarity of two time-series data was used. The normalized cross-correlation function of two time-series data (x and y) is.

$$r_{\{x,y\}}(k) = \frac{\sum_{i=1}^{k}\left(x_i - \bar{x}\right)\left(y_{i+N-k} - \bar{y}\right) + \sum_{i=k+1}^{N}\left(x_i - \bar{x}\right)\left(y_{i-k} - \bar{y}\right)}{\sqrt{\sum_{i=1}^{N}\left(x_i - \bar{x}\right)^2}\sqrt{\sum_{i=1}^{N}\left(y_i - \bar{y}\right)^2}}$$

(9)

where $\bar{x}$ and $\bar{y}$ denotes the mean values of those two time-series data. k means a phase shift of one signal and N is the total number of data points of one signal. The maximum cross-correlation value of 1 indicates that the two corresponding signals are identical. The maximum cross-correlation values of left and right knee angles were calculated shown in Table 4. When a motor helps the patient walk on the robot in the assisted-active mode, the maximum

Table. 4 Maximum cross-correlation values of left and right knee angular displacement for the two training modes

Assisted-active mode	Active mode
0.993 ± 0.003	0.935 ± 0.042

Fig. 18 Snapshots of a walking experiment

cross-correlation values were higher than in the active mode (Table 4). This result suggests that the robot effectively help the patient walk normally by leading to laterally symmetric gait patterns. Figure 18 shows the snapshots of walking experiment.

5 Conclusion

In this paper, we proposed three rehabilitation modes of end-effector type hybrid gait rehabilitation robots and verified the performance of training modes experimentally. The advantages and the hardware characteristics of the developed gait rehabilitation robot were described in comparison with the existing gait rehabilitation robots. The motor driving principle and the speed profile of the proposed gait training modes were proposed. Lastly, the EMG signal measurement experiment was performed to confirm the muscle auxiliary performance at each training mode, and the improved motion of the affected limb was experimentally verified using the IMU based motion capture experiment.

To examine the hardware operation performance of the developed robot and the effectiveness of the proposed algorithm, we conducted the experiment. In the near future, we plan to improve the hardware and software of the robot through the usability evaluation of the patients. In the long term, we plan to upgrade the developed robot steadily in consideration of safety and reliability for medical device certification.

References

1. Kim, K. E., Park, W. B., Oh, M. K., Kang, E. K., Lim, J. Y., Yang, E. J., et al. (2010). The effect of physical performance and physical activity on quality of life in old people: The Korean longitudinal study on health and aging. *Annals of Geriatric Medicine and Research,14*(4), 212–220.
2. Kelly-Hayes, M. (2010). Influence of age and health behaviors on stroke risk: Lessons from longitudinal studies. *Journal of the American Geriatrics Society,58*(S2), S325–S328.
3. Reeve, A., Simcox, E., & Turnbull, D. (2014). Ageing and Parkinson's disease: Why is advancing age the biggest risk factor? *Ageing Research Reviews,14*, 19–30.
4. Thorsén, A. M., Holmqvist, L. W., de Pedro-Cuesta, J., & von Koch, L. (2005). A randomized controlled trial of early supported discharge and continued rehabilitation at home after stroke five-year follow-up of patient outcome. *Stroke,36*, 297–302.
5. Bernhardt, J., Dewey, H., Thrift, A., Collier, J., & Donnan, G. (2008). A very early rehabilitation trial for stroke (AVERT) phase II safety and feasibility. *Stroke,39*, 390–396.
6. Belda-Lois, J. M., Horno, S. M., Bermejo-Bosch, I., Moreno, J. C., Pons, J. L., Farina, D., et al. (2011). Rehabilitation of gait after stroke: A review towards a top-down approach. *Journal of NeuroEngineering and Rehabilitation,8*, 66.
7. Eng, J. J., & Tang, P. F. (2007). Gait training strategies to optimize walking ability in people with stroke: A synthesis of the evidence. *Expert Review of Neurotherapeutics,7*(10), 1417–1436.
8. Ko, C. Y., Ko, J. W., Kim, H. J., & Lim, D. H. (2016). New wearable exoskeleton for gait rehabilitation assistance integrated with mobility system. *International Journal of Precision Engineering and Manufacturing,17*(7), 957–964.
9. Hidler, J., Brennan, D., Black, I., Nichols, D., Brady, K., & Nef, T. (2018). Master–slave control of an intention-actuated exoskeletal robot for locomotion and lower extremity rehabilitation. *International Journal of Precision Engineering and Manufacturing,19*(7), 983–991.
10. Hidler, J., Brennan, D., Black, I., Nichols, D., Brady, K., & Nef, T. (2011). ZeroG: Overground gait and balance training system. *Journal of Rehabilitation Research and Development,48*(4), 287–298.
11. Jezernik, S., Colombo, G., Keller, T., Frueh, H., & Morari, M. (2003). Robotic orthosis lokomat: A rehabilitation and research tool. *Neuromodulation,6*(2), 108–115.
12. Kim, S. Y., Yang, L., Park, I. J., Kim, E. J., JoshuaPark, M. S., You, S. H., et al. (2015). Effects of innovative WALKBOT robotic-assisted locomotor training on balance and gait recovery in hemiparetic stroke: A prospective, randomized, experimenter blinded case control study with a 4-week follow-up. *IEEE Transactions on Neural Systems and Rehabilitation Engineering,23*(4), 636–642S.
13. Hesse, A., & Waldner, C. Tomelleri. (2010). Innovative gait robot for the repetitive practice of floor walking and stair climbing up and down in stroke patients. *Journal of Neuroengineering and Rehabilitation,7*, 30.
14. Kim, J. J., Kim, M. J., Kwak, N. S., Kim, C. H., Kim, H., & Kim, J. Y. (2018). Development of an end-effector typed walking rehabilitation robot capable of power assistance. *Transactions of the KoreanSociety of Mechanical Engineers - A,42*(8), 721–730.
15. Mehrholz, J., Wagner, K., Rutte, K., Meibner, D., & Pohl, M. (2007). Predictive validity and responsiveness of the functional ambulation category in hemiparetic patients after stroke. *Archives of Physical Medicine and Rehabilitation,88*, 1314–1319.
16. Hesse, S., Werner, C., Paul, T., Bardeleben, A., & Chaler, J. (2001). Influence of walking speed on lower limb muscle activity and energy consumption during treadmill walking of hemiparetic

patients. *Archives of Physical Medicine and Rehabilitation,88*(11), 1547–1550.

17. Gait training algorithm of an end-effector typed hybrid walking rehabilitation robot. (2019). https://youtu.be/K-YhacSxjZk. Accessed March 6, 2019.

18. Hsiao-Wecksler, E., Polk, J., Rosengren, K., Sosnoff, J., & Hong, S. (2010). A review of new analytic techniques for quantifying symmetry in locomotion. *Symmetry,2*(2), 1135–1155.

Publisher's Note Springer Nature remains neutral with regard to jurisdictional claims in published maps and institutional affiliations.

Jung-Yup Kim received his B.S and M.S degrees in Mechanical Engineering from INHA University, Incheon, South Korea, and Ph.D. degree in Mechanical Engineering from Korea Advanced Institute of Science and Technology (KAIST), Daejeon, South Korea, in 1999, 2001 and 2006, respectively. He was a Post Doctor of Humanoid Robot Research Center at KAIST and Robotics Institute of Carnegie Mellon University, Pittsburgh, U.S.A in 2006 and 2007 respectively. Since 2008, he has been a Professor in Department of Mechanical System Design Engineering of Seoul National University of Science and Technology, Seoul, South Korea. His research interests include mechanical design, motion planning and dynamics control of legged robots, rehabilitation/assistive/prosthetic robots, and smart robotics bike. He is a member of the Korea Society of Mechanical Engineers (KSME), the Korean Society for Precision Engineering (KSPE), and Korea Robotics Society (KROS) in Korea.
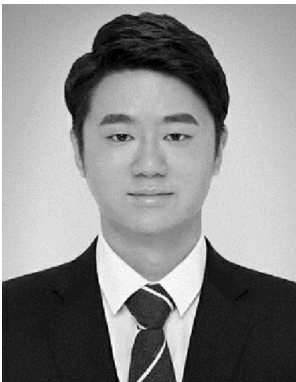
Jung-Joon Kim received his B.S degrees in Department of Mechanical System Design Engineering from Seoul National University of Science and Technology, Seoul, South Korea in 2017. Since 2017, he is a M.S degree student in Department of Mechanical Design and Robot Engineering from Seoul National University of Science and Technology, Seoul, South Korea. His research interests include mechanical optimization design, motion profile design, training algorithms of gait rehabilitation robot.

Kiwon Park joined the department of Mechatronics Engineering at Incheon National University, Korea in 2018 as Associate Professor. He had worked as Assistant Professor and Associate Professor at the department of Mechanical and Aerospace Engineering at Trine University, USA after receiving his Ph.D. in Mechanical Engineering from the University of Illinois at Urbana-Champaign. He received his M.S. in Engineering Mechanics from Virginia Polytechnic Institute and State University (Virginia Tech). He obtained his B.S. from Inha University, Korea in Mechanical Engineering. Dr. Park's studies focus on rehabilitation robotics, the dynamical/biomechanical analysis of human body motions and the development of a new technique to characterize coupled joint patterns in the human gait.